*J. Fluid Mech.* (1972), *vol.* 52, *part* 3, *pp.* 451–464
*Printed in Great Britain*



# Laminarization of turbulent pipe flow by fluid injection

By W. T. PENNELL, E. R. G. ECKERT AND E. M. SPARROW
University of Minnesota, Minneapolis

(Received 4 May 1971 and in revised form 15 November 1971)

The effects of fluid injection on the structure of an initially fully developed, low Reynolds number, turbulent pipe flow have been studied by means of a hot-film anemometer. Measurements were made of the axial turbulence intensity field and of the time-mean streamwise velocity distribution, both in the porous-walled pipe and in the solid-walled hydrodynamic development section. Oscilloscope traces showing the timewise pattern of the local velocity fluctuations were also monitored. The Reynolds number of the air flow at the inlet of the porous pipe was varied from 3090 to 6350, and the Reynolds number of the injected air ranged from 60 to 160.

Near the tube wall, the initial effect of injection is a significant reduction of the axial turbulence level and an increase in the thickness of the viscous and buffer layers. The degree by which turbulence is reduced in this region is more or less proportional to the ratio of the injection to entrance Reynolds numbers. In the core region of the flow, which is centred about the tube axis, there is also an initial reduction in the magnitude of the axial component of turbulence which is thought to be due to injection-induced acceleration of the flow. There is also an annular region, which separates the wall and core regions, in which the turbulence intensity initially increases. In the downstream portion of the porous tube the entire flow undergoes a re-transition to fully developed turbulence.

## 1. Introduction

Flows with mass addition or mass withdrawal at the bounding surfaces form a class of technologically important problems. Extensive experimental and analytical research has been conducted into the fluid mechanics of such problems. For internal flows with surface mass transfer, which is the area of interest of this paper, most of the published research has been directed toward laminar conditions.

The present research is concerned with turbulent flow in a porous-walled circular tube and, in particular, with the effect of surface mass transfer on the structure of the turbulence. In the experimental arrangement a low Reynolds number turbulent air flow (i.e. the main flow) was passed through a solid-walled hydrodynamic development section and thence into the porous tube. The effects of secondary air injection at the tube wall were investigated by hot-film anemometry. Radial and axial distributions of turbulence intensity and time-mean velocity were measured for various combinations of the main-flow Reynolds

number and the injection-flow Reynolds number. Oscilloscope traces were observed and photographed with a view to exploring the timewise behaviour of the local velocity fluctuations.

The present investigation was largely motivated by the results of a recent experimental study by Huesmann & Eckert (1968) of developed laminar tube flow with uniform injection. The experimental set up was similar to that depicted in figure 1, except that the entrance of the porous tube was sealed off by a plug. Thus flow was generated by injection only. Starting with rather low values of the injection Reynolds number, $Re_w = V_w D/\nu$, Huesmann & Eckert measured both the laminar flow velocity profile and the static pressure at various axial stations in the tube. These measurements were repeated for increasingly large rates of injection in order to determine the transition Reynolds number. The effects of injection on the flow were found to be stabilizing since transition was not detected until a local main-flow Reynolds number of 10000 was reached.

These results prompted an inquiry into the effects of injection on low Reynolds number turbulent pipe flow entering a porous tube. Of particular interest was the question of whether injection would result in a tendency for the flow to revert to the laminar state. In an initial attempt to examine this matter, Eckert & Rodi (1968) conducted impact probe measurements of velocity distributions in a porous tube for a number of injection rates and for various low Reynolds number turbulent entrance conditions. These measurements revealed noteworthy changes in the shape factor

$$\beta = \int_A U^2 dA / U_{\mathrm{av}}^2 A$$

as a result of injection. It was found that in the entrance region $\beta$ increased significantly with axial position (approaching values associated with laminar flow), reached a maximum and then decreased. This behaviour seemed to indicate a tendency towards laminarization in the entrance region which is then followed by a re-transition to developed turbulent flow.

Measurements such as the ones mentioned above, however, are not capable of sensing the effects of injection on the structure of the turbulence during the apparent laminarization and re-transition. Such information can only be provided by direct measurements of the relevant turbulence quantities themselves. The present study was undertaken to obtain and report such turbulence measurements.

Inasmuch as heat-transfer processes are strongly influenced by the structure of the turbulence adjacent to a wall, the results reported here should have implications for heat transfer in transpiration-cooled tube flows.

## 2. Apparatus

The experimental apparatus used in the research will be described here in general terms, detailed information being available in the thesis (Pennell 1970) from which this paper is drawn.

A schematic of the porous tube test section and its surrounding plenum chamber is given in figure 1. Clean compressed air, free of water and oil, was

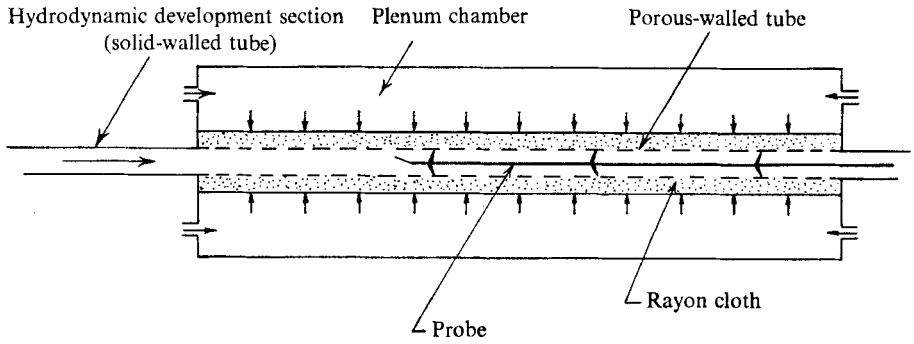


FIGURE 1. Schematic of the porous tube test section and its surrounding plenum chamber.

conveyed to the inlet of the porous-walled tube by means of a seamless brass pipe (35·5 mm in diameter, 90 diameters long) which served as a hydrodynamic development section. The development section was carefully aligned with the porous tube in order to eliminate extraneous velocities induced by pipe curvature. Air was supplied to the plenum chamber surrounding the porous test section through four inlet ports. The plenum air passed radially inward through the porous wall and into the tube bore.

The heart of the experimental apparatus was the porous tube 35·5 mm in diameter and just over 24 diameters in length. The tube was manufactured by the Bendix Filter Division, Bendix Aviation Corporation from a material known commercially as Porastrand. Owing to the relatively high permeability of the porous material, it was necessary to increase the flow resistance across the tube wall to ensure that the local injection rate would be insensitive to the axial pressure drop of the main flow. This was accomplished by wrapping the outside of the porous pipe with approximately eighty layers of densely woven rayon cloth. Evidence as to the uniformity of the injected flow along the length of the tube will be given later. With respect to the smoothness of the inside surface of the porous tube, friction factor measurements implied a roughness approximately equal to that of a commercial steel pipe (Olson 1964).

Local measurements were made to determine the axial turbulent velocity fluctuations and the time-mean axial velocity. The measurements were performed at various radial positions in cross-sections spanning most of the length of the porous tube and also extending back into the hydrodynamic development tube. The data were acquired with the aid of a Thermo Systems model 1275 miniature probe equipped with a model 10A cylindrical hot-film sensor and used in conjunction with a Thermo Systems 1050 series constant-temperature anemometer. The sensor had a diameter of 0·025 mm and an effective sensing length of 0·25 mm. The calibration of the sensor is described elsewhere (Pennell 1970). A hot-film sensor was chosen in preference to a hot wire for two basic reasons. First, the hot-film sensor, owing to its larger diameter, is much stronger and thus less prone to breakage; second, the shorter sensing length of the hot-film sensor results in better spatial resolution.

The sensor was installed in the traversing mechanism with the axis of the

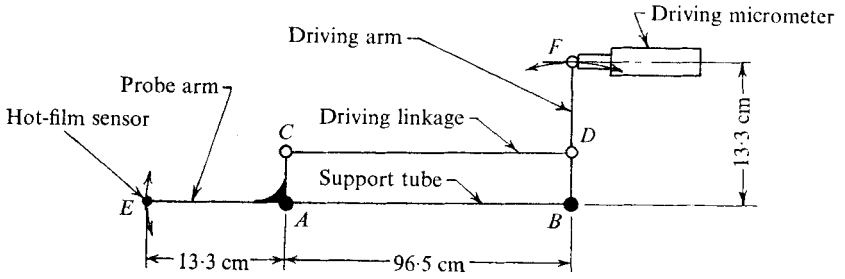


FIGURE 2. Schematic of the mechanism for positioning the velocity sensor. ●, fixed pivot points; ○, movable pivot points.

sensor perpendicular to the direction of radial traverse and also perpendicular to the axial direction. This orientation was chosen both to allow measurements to be made closer to the tube wall and to minimize variations of velocity along the sensing surface. The principle drawback of this orientation is the increased sensitivity to the radial velocity component. However, since the blowing velocities employed in this work were quite low ( $< 0{\cdot}072$ m/s), the contribution of the radial velocity component to the effective cooling velocity acting on the sensor was negligible (Pennell 1970, appendix A). For all practical purposes the sensor could be considered as responding only to the axial velocity component.

For practical reasons related to the porous nature of the tube and to the large number of cross-sections to be surveyed, the probe and traversing mechanism were introduced into the flow from the exit end of the tube (see figure 1). This arrangement meant that the controls for manipulating the motion of the probe had to be located at a considerable distance from the probe itself. Figure 2 is a schematic of the mechanism which was designed and fabricated for positioning the sensor in the porous tube. The device is, in essence, a symmetrical four-bar mechanism in which the probe arm and the driving arm are connected through a driving linkage. The probe arm pivots around point $A$ and moves in response to movements of the driving micrometer. The distances $AC$ and $BD$ were made equal so that movement of the driving arm through a certain angle would cause a movement of the probe arm through an equal angle. By adjustment of the length of the arm, $BF$, the movement of the sensor was made to agree to within 0·02 mm with the movement indicated by the driving micrometer. The support tube $AB$ of the traversing mechanism was fitted with rigid and spring struts to ensure accurate positioning along the centre-line of the tube.

The radial position of the sensor was based on the distance from the wall, which was established with the aid of an electrical contact mechanism (Pennell 1970). Because the traversing mechanism moved the sensor through an arc, the axial position of the sensor did not remain constant during a radial traverse, but varied by 1·1 mm between the centre-line and the closest approach to the wall. Since this variation corresponds to only 0·03 tube diameters it was ignored. Positioning of the sensor at the various cross-sections of interest was accomplished by sliding the entire traversing mechanism farther into (or out of) the porous tube.

The experimental data were reduced by means of a hybrid computer in on-line operation. The hybrid system consisted of an EAI 680 analog computer coupled

by an analog–digital interface to a CDC 1700 digital computer. The analog computer was used primarily as a variable time constant r.m.s. voltmeter. The digital computer was programmed to operate the analog computer; to collect, store and print-out the raw data; to perform the necessary calculations required to convert the raw data into the desired physical quantities; and to print out these results. Specifically, at each probe location the computer output provided the time-mean axial velocity and the root-mean-square value of the fluctuations in the axial velocity.

## 3. Presentation of results

The operating conditions of the experiments were characterized by the main-flow Reynolds number at the inlet of the porous tube ($Re_0$) and the injection Reynolds number ($Re_w$). The ranges of these parameters that were covered during the course of the research are listed in table 1.

| | | | | | | | | | | | | |
|---|---|---|---|---|---|---|---|---|---|---|---|---|
| $Re_0$ | 5850 | 5630 | 5850 | 6350 | 4540 | 4150 | 4340 | 4250 | 3200 | 3200 | 3090 | 3090 |
| $Re_w$ | 60 | 90 | 120 | 160 | 70 | 90 | 120 | 160 | 60 | 100 | 110 | 150 |

TABLE 1. Ranges of $Re_0$ and $Re_w$

The main-flow Reynolds number $Re$ at an axial station situated at a distance $x$ downstream of the inlet of the porous tube can be expressed in terms of $Re_0$ and $Re_w$ as

$$Re = Re_0 + 4(x/D)Re_w, \tag{1}$$

where $$Re = U_{\mathrm{av}}D/\nu, \quad Re_0 = U_{\mathrm{av},0}D/\nu, \quad Re_w = V_wD/\nu.$$

$U_{\mathrm{av}}$ and $U_{\mathrm{av},0}$ are, respectively, the cross-sectionally averaged, time-mean velocities at $x = x$ and $x = 0$, whereas $V_w$ is the injection velocity at the wall. In view of (1), it is seen that there is an appreciable increase in the Reynolds number along the length of the porous tube.

For each operating condition radial traverses were performed at six to eleven different axial stations, depending on the particular case. Typically, four radial traverses were made in each cross-section at circumferential locations corresponding to the 3, 6, 9 and 12 o'clock directions. At each point of a traverse four consecutive measurements were made and averaged.

The output of the anemometer was analysed by means of a linear model wherein approximations were introduced under the assumption that the local turbulence intensity is small compared with the local time-mean velocity. It appears that such an analysis gives rise to turbulence intensity values that are somewhat higher than those actually existing in the flow (Pennell 1970, appendix A). In the present research, there were certain extreme cases where modest quantitative errors were sustained as a result of the linearized analysis. However, in no case was there any effect on the essential qualitative trends.

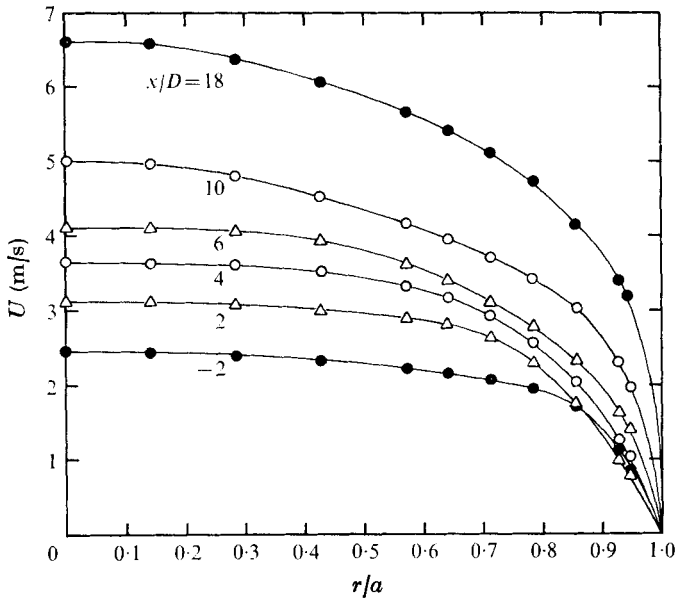


FIGURE 3. Representative time-mean velocity profiles at a succession of axial stations; $Re_0 = 4150$, $Re_w = 90$.

### 3.1. *Time-mean velocity measurements*

Before beginning the study of the effects of injection on the structure of the turbulence, some preliminary measurements which repeated some of the experiments of Huesmann & Eckert (1968) for laminar flow and of Eckert & Rodi (1968) for the time-mean turbulent velocity field were made. The purpose of these experiments was to assess the accuracy and reliability of the measurement technique. Excellent agreement was obtained, over the entire tube cross-section, between the hot-film anemometer measurements and the results of the earlier investigators, all of whom used static-impact pressure probes for determining the velocity profiles.

A representative set of axially developing velocity profiles, measured by the hot-film anemometer, is presented in figure 3. These results, which represent averages taken over the four quadrants of the tube at each axial station, are for an entrance Reynolds number of 4150 and an injection Reynolds number of 90. Curves have been faired through the data points to enhance the clarity of the figure. As can be seen from the figure, a particularly noteworthy effect of injection on the time-mean velocity profile is a reduction in the velocity gradient at the wall in the entrance region of the porous tube. This reduction in the velocity gradient, however, does not persist for more than a few diameters.

In figure 4, cross-sectionally averaged, time-mean velocities are plotted as a function of $x/D$ for several injection Reynolds numbers and an entrance Reynolds number of approximately 4000. This figure is typical of those for the other entrance Reynolds numbers studied. For uniform injection, a plot of cross-sectionally averaged mean velocity as a function of $x/D$ will yield a straight line; thus, plots such as these serve to indicate the uniformity of injection. As the

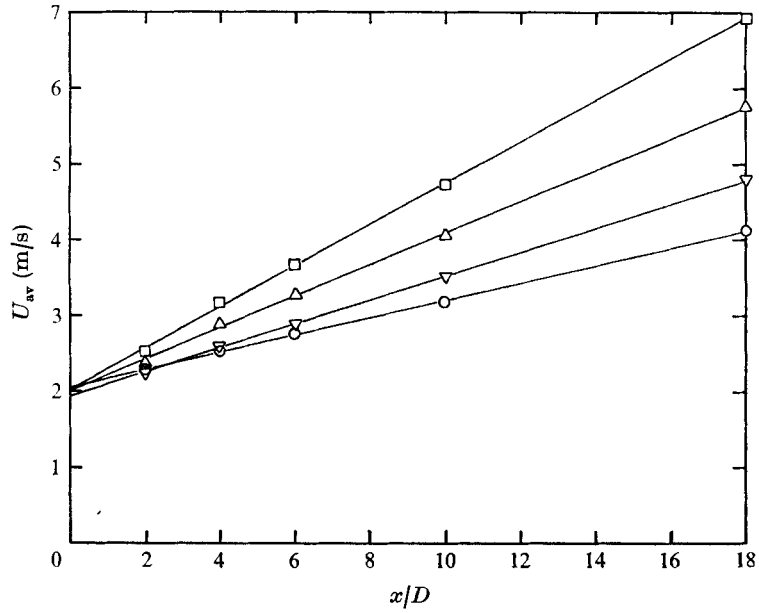


FIGURE 4. Axial distributions of cross-sectionally averaged, time-mean velocities. $Re_0 \sim 4000$; ○, $Re_w = 70$; ▽, $Re_w = 90$; △, $Re_w = 120$; □, $Re_w = 160$.

figure shows, the injection was indeed uniform along the length of the tube. For the combinations of entrance and injection Reynolds numbers employed in this research the data points deviate by no more than $\pm 2\,\%$ from a straight line faired through the points.

### 3.2. *Time records of the fluctuating velocity field*

Figures 5 and 6 (plates 1–4) are photographs of oscilloscope traces of the hot-film output for two specific combinations of entrance and injection Reynolds numbers: $Re_0 = 3200$, $Re_w = 160$, and $Re_0 = 4200$, $Re_w = 160$, respectively. The probe orientation was such as to measure the axial velocity. Each figure has two parts, (*a*) and (*b*), showing results for $x/D = -2, 1, 4$ and for $x/D = 6, 12, 18$ respectively. Each column is for a given $x/D$ and the photos are vertically arranged according to the radial co-ordinate $r/a$.

The photographs in figures 5 (*a*) and (*b*) (plates 1 and 2) depict the nature of the flow for the combination of entrance and injection Reynolds numbers ($Re_0 = 3200$, $Re_w = 160$) for which the greatest effect of injection on the entering flow was encountered. The first column of photographs shows the structure of the turbulence in the low Reynolds number flow entering the porous section. At the next axial station, $x/D = 1$, a drastic reduction in turbulence level in the region near the tube wall is indicated. At $r/a = 0{\cdot}928$ the flow appears to be nearly laminar (although some very low amplitude disturbances are still evident). There is also a substantial reduction in turbulence level at $r/a = 0{\cdot}857$ ($\sim 2{\cdot}5$ mm from the tube wall); however, this reduction is not nearly as great as at the previously mentioned location. At the next radial position, $r/a = 0{\cdot}785$, only a slight reduction in the

magnitude of the turbulent fluctuations is apparent. It would appear that at this position the main flow is just beginning to feel the effects of surface mass transfer. In the region near the tube centre-line ($r/a = 0{\cdot}428$ and $r/a = 0$), only a slight reduction in turbulent intensity is shown.

At $x/D = 4$, amplification of selective disturbances is becoming evident at $r/a = 0{\cdot}928$. It is the growth of disturbances such as these which ultimately results in the breakdown of the near-laminar flow in the wall region. In the photographs at the next axial station, $x/D = 6$, the process of re-transition to turbulence is further illustrated. At $r/a = 0{\cdot}928$ the amplified disturbances, of which the photograph shows a typical specimen, have grown considerably in strength and taken on the character of turbulent bursts, giving the flow a somewhat intermittent character. Disturbances of a quite similar nature can be seen at $r/a = 0{\cdot}857$ and $r/a = 0{\cdot}785$, although these bursts are imbedded in a matrix of somewhat more highly disturbed flow.

At $x/D = 10$ the flow is entering the latter stages of re-transition. As indicated by the photographs corresponding to $r/a = 0{\cdot}928$ and $0{\cdot}857$, high amplitude, higher frequency disturbances are becoming more common, and the flow between these bursts is becoming more disturbed. Breakdown of the flow at $r/a = 0{\cdot}785$ is in an even more advanced stage. Once the breakdown of the flow is under way, there seems to be an almost explosive increase in the frequency of the turbulence. From the photograph at $r/a = 0{\cdot}428$ it can be seen that these high frequency, high intensity bursts have also begun to appear in regions nearer the tube centre-line. By the time that the flow has progressed 18 diameters down the porous pipe, the turbulent flow field appears to have become fully developed. At this axial station, the local main-flow Reynolds number is approximately 14700.

In figures 6(*a*) and (*b*) (plates 3 and 4) photographs depicting the effects of injection on turbulent flow for a somewhat smaller ratio of injection to entrance Reynolds number are shown. As can be seen from an overall appraisal of the figures, laminarization brought about by injection is not as complete as in the previously discussed case. In addition, it is apparent that re-transition occurs more rapidly.

### 3.3. *Effects of injection on turbulence intensity*

In figures 7–9 r.m.s. values of the axial velocity fluctuations are plotted as a function of axial position for several radial locations.† The time-mean centre-line velocity at the inlet section, $U_{0,c}$, is used to provide dimensionless results. Since $U_{0,c}$ is not a function of $x/D$ these figures indicate how, at a given radial position, $u'$ varies as the flow moves down the pipe. Each figure corresponds to one of the three entrance Reynolds numbers which were studied, i.e. $Re_0 \sim 6000$, $Re_0 \sim 4400$ and $Re_0 \sim 3100$. In each figure, graphs are presented for both the lowest and the highest injection rates studied.

The figures contain results for five (or six) radial positions. The plotted points represent averages taken over the four quadrants of the tube (i.e. from traverses along the 3, 6, 9 and 12 o'clock directions), except for the graphs corresponding to

† The symbol $u'$ is used here as an abbreviation for $(\overline{u^2})^{\frac{1}{2}}$, where $u$ is the fluctuating portion of the axial velocity.

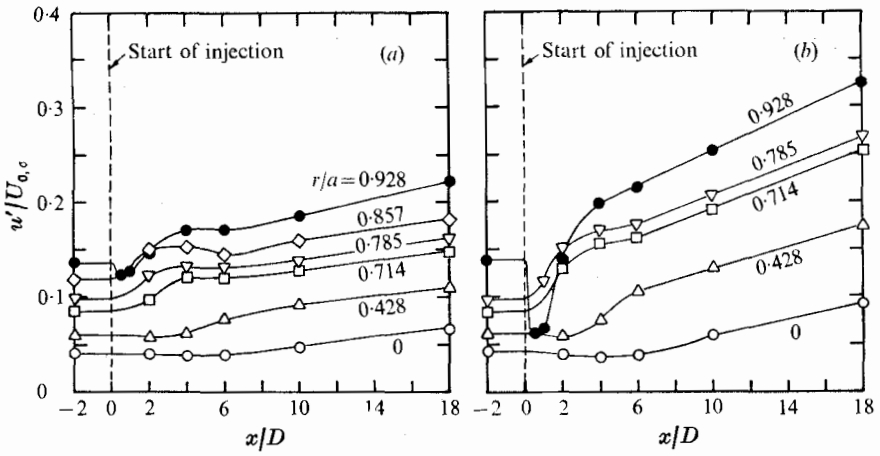


FIGURE 7. Axial distributions of r.m.s. velocity fluctuations at several radial positions, $Re_0 \sim 6000$. (*a*) $Re_0 = 5850$, $Re_w = 60$, (*b*) $Re_0 = 6350$, $Re_w = 160$.

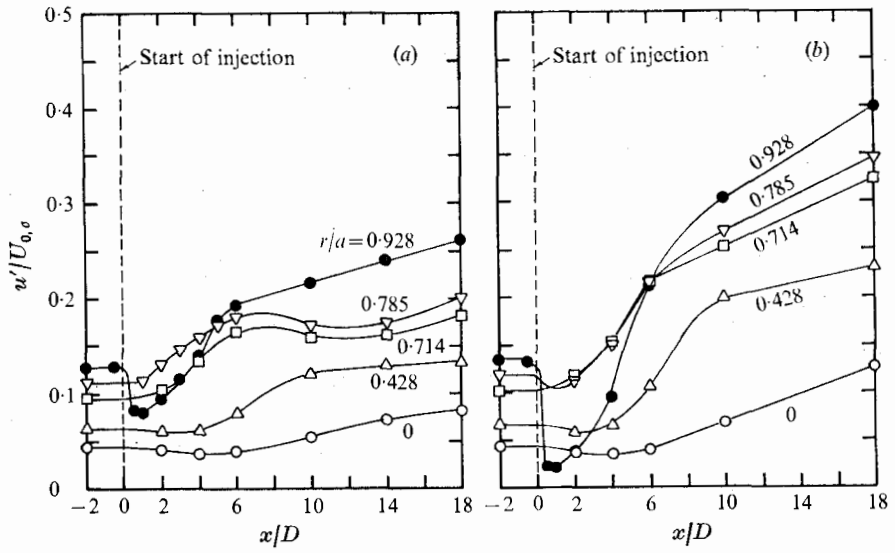


FIGURE 8. Axial distributions of r.m.s. velocity fluctuations at several radial positions, $Re_0 \sim 4400$. (*a*) $Re_0 = 4540$, $Re_w = 60$, (*b*) $Re_0 = 4250$, $Re_w = 160$.

the highest injection rates in figures 8 and 9. For these cases the plotted points represent measurements made in the lower quadrant of the tube (i.e. along the 6 o'clock direction).

For those combinations of entrance and injection Reynolds numbers where the turbulence was most drastically affected by injection, a noticeable circumferential asymmetry in the flow was observed near the tube wall in the entrance region. The greatest degree of asymmetry was found for the highest ratio of injection to entrance Reynolds number ($Re_w = 150$ and $Re_0 = 3090$, figure 9(*b*)). For this case it was observed that, adjacent to the wall, injection resulted in an almost total elimination of turbulent fluctuations within one diameter after the start of injection in all but the upper quadrant. From measurements performed in the

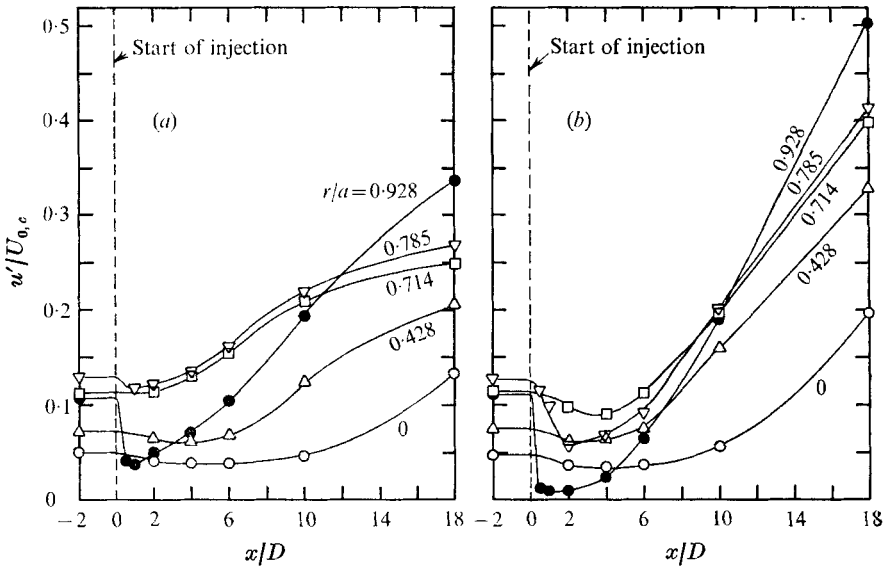


FIGURE 9. Axial distributions of r.m.s. velocity fluctuations at several radial positions, $Re_0 \sim 3100$. (a) $Re_0 = 3200$, $Re_w = 60$, (b) $Re_0 = 3090$, $Re_w = 150$.

absence of injection, no discernible changes in $u'$ were found to occur when the flow passed from the hydrodynamic development section to the porous tube. Therefore, the aforementioned asymmetry was somehow connected with the injection and not with irregularities in the entrance geometry.

At the highest ratio of injection to entrance Reynolds number (figure 9(*b*)), extensive probing with the hot-film sensor around the circumference of the tube at $x/D = \frac{1}{2}$ and $r/a = 0{\cdot}928$ revealed a region of relatively high disturbance in the upper quadrant and covering roughly $\frac{1}{6}$ of the tube circumference. At lower $Re_w/Re_0$ values (figure 8 (*b*)) the region of disturbance was smaller and the resulting asymmetry in $u'$ less marked. For all the other combinations of entrance and injection Reynolds numbers no significant asymmetry was observed.

For those cases exhibiting significant asymmetry, plots of $u'$ as a function of $x/D$ for each tube quadrant showed that, in the lower quadrant, the downstream flow was least affected by the disturbance originating in the upper quadrant (Pennell 1970). Thus, in these cases, turbulence measurements from the lower quadrant are plotted since it is felt that they most closely represent the behaviour which would occur in the absence of the asymmetry just discussed.

Inspection of figures 7–9, especially the graphs corresponding to the higher entrance Reynolds numbers (6000 and 4000), indicates that the flow in the entrance region of the porous tube may be divided into three zones: (i) a wall region extending from the tube wall to $r/a = 0{\cdot}928$ or $0{\cdot}785$ (depending upon the ratio $Re_w/Re_0$), (ii) a core region centred about the tube centre-line, (iii) an annular region lying between the core and the wall regions. At the lowest entrance Reynolds number this division is not so distinct.

The effect of injection on the turbulence level in the wall region is almost immediate. There is a precipitous drop in $u'$ just downstream of the beginning of

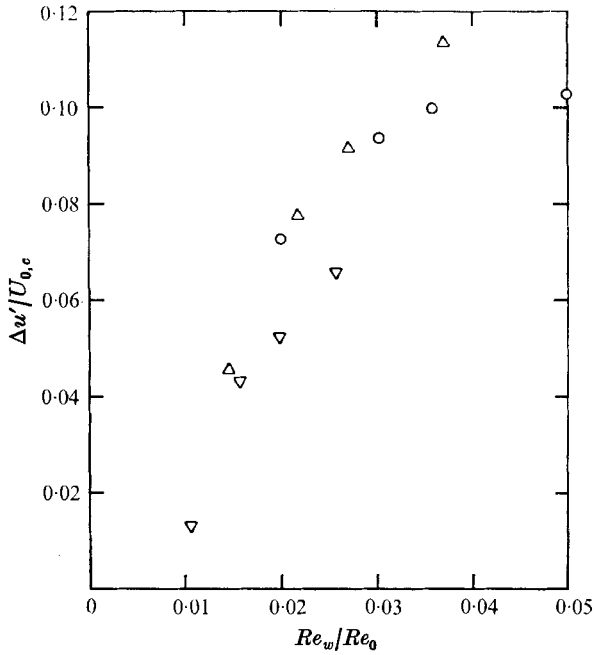


FIGURE 10. Reduction in $u'$ at $r/a = 0{\cdot}928$ due to injection.
○, $Re_0 = 3100$; △, $Re_0 = 4300$; ▽, $Re_0 = 6000$.

injection (the minimum being attained within one tube diameter) and the degree to which turbulence is reduced in this region increases with increasing $Re_w/Re_0$. After the minimum has been reached, the near-laminar flow breaks down and rapidly approaches fully turbulent conditions. The laminarization and subsequent re-transition shown in figures 7–9 is in accord with that indicated in the photographs of figures 5 and 6.

The relationship between the reduction in $u'$ and the $Re_w/Re_0$ ratio is shown in figure 10. In the figure, $\Delta u'/U_{0,c}$ (with $\Delta u' = u'_{-2} - u'_1$) as measured at $r/a = 0{\cdot}928$ is plotted as a function of $Re_w/Re_0$. The correlation of the results for the various combinations of entrance and injection Reynolds numbers appears to be reasonably good.

The aforementioned reduction of the turbulence level in the wall region is believed to be due to the injection of fluid which is in the laminar state. The injected fluid seeps out through tiny pores such that the Reynolds number based on the pore size and pore velocity is very small. At these low Reynolds numbers, the injected fluid leaves the wall without flow separation or vortex formation. This laminar injection should thicken the viscous dominated sublayer in the entrance region. Both the thickness and persistence of the layer are increased at larger values of $Re_w/Re_0$.

In the core region, represented in figures 7–9 by the curves at $r/a = 0$ and $0{\cdot}428$, $u'$ at first decreases with $x/D$ reaching a minimum, and then increases as fully developed flow conditions are approached. The decrease in $u'$ is substantially less marked than in the wall region. At the centre-line, the minimum in $u'$ occurs about four diameters from the start of injection, with the degree of change

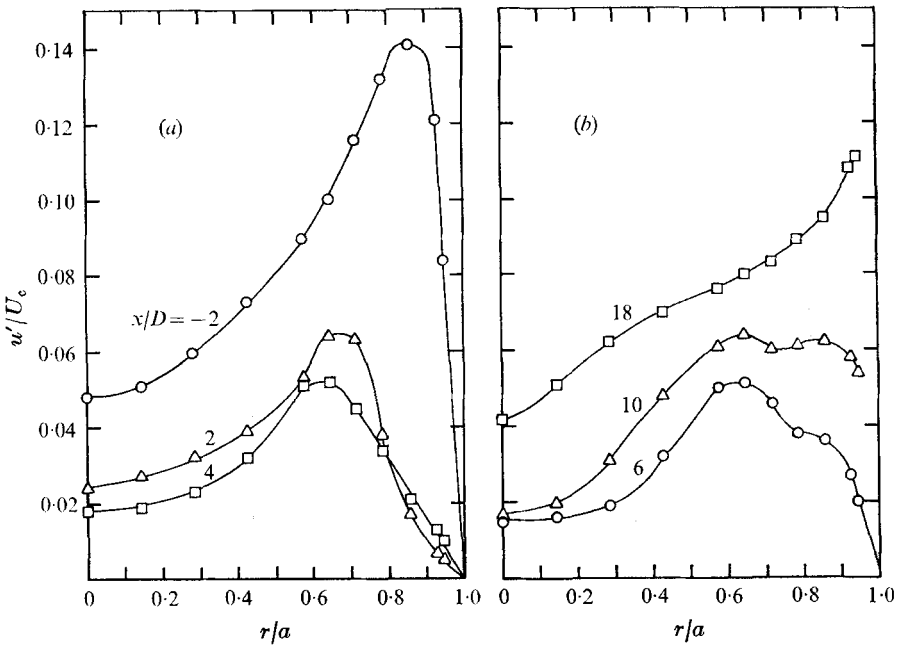


FIGURE 11. Profiles of r.m.s. velocity fluctuations at a succession of axial stations; $Re_0 = 3090$, $Re_w = 150$. (*a*) Entrance region. (*b*) Downstream region.

in $u'$ depending on the ratio $Re_w/Re_0$. At $r/a = 0{\cdot}428$ the flow reacts somewhat more quickly to injection.

Owing to injection, the centre-line time-mean velocity increases in the streamwise direction. It is an established fact that, in general, a flow acceleration decreases the magnitude of the fluctuations in the streamwise direction (Batchelor 1953). Such an effect is in evidence in the entrance region of the porous tube. The reversal of this trend, i.e. the increase in turbulence in the downstream part of the porous tube, is probably due to transport of turbulent kinetic energy toward the centre-line from the regions of the flow which lie nearer the wall.

At the higher entrance Reynolds numbers ($Re_0 \sim 4000$ and 6000), there is a distinct annular region (separating the wall and core regions of the flow) in which $u'$ undergoes an initial increase in magnitude instead of an initial reduction in magnitude. This region is represented in figures 7 and 8(*a*) by the curves corresponding to $r/a = 0{\cdot}857$, $0{\cdot}785$ and $0{\cdot}714$, and in figure 8(*b*) by the curve for $r/a = 0{\cdot}714$. At the lowest entrance Reynolds number a distinct annular region is discernible only for the lowest injection Reynolds number (figure 9(*a*)).

After the initial increase mentioned above, and for some combinations of $Re_0$ and $Re_w$, $u'$ reaches a plateau on which there is little or no increase in the level of turbulence. Then the intensity of the turbulence begins to increase again as fully developed conditions are approached; however, this increase is at a much slower rate. For some cases, the $u'$ plateau is followed by a slight decrease in the level of turbulence (e.g. figures 7(*a*) and 8(*a*)). This behaviour of $u'$ was so unusual that the measurements were repeated and verified several times over a period of many months.

### 3.4. *Profiles of turbulence intensity*

In figure 11, the effect of injection on the turbulence is presented from another point of view. The r.m.s. axial component of turbulent velocity $u'$, normalized by the local centre-line velocity $U_c$, is plotted as a function of $r/a$ for various axial stations and for the combination of entrance and injection Reynolds numbers $Re_0 = 3090$ and $Re_w = 150$, which corresponds to the largest value of $Re_w/Re_0$ studied. The sudden thickening of the viscous dominated regions of the flow due to the start of injection is illustrated quite clearly in the figure. The maximum turbulence intensity moves from $r/a = 0{\cdot}86$ at $x/D = -2$ to $r/a = 0{\cdot}62$ at $x/D = 2$.

As the flow moves downstream and begins to approach fully developed conditions the region of high turbulence intensity begins to spread transversely. In the later stages of the re-transition process ($x/D = 6$ and $x/D = 10$) the turbulence intensity profiles develop a rather curious double-humped shape. This behaviour was observed for several other combinations of entrance and injection Reynolds numbers, becoming more pronounced at larger values of $Re_w/Re_0$ (Pennell 1970). It would seem that the double-humped profile is a definite characteristic of the re-transition process. The hump nearest the wall is believed to result from the breakdown of the laminar layer.

In turbulent flow through a tube without fluid injection, the turbulence intensity reaches its largest value close to the wall. This can be observed from the curve for $x/D = -2$ in figure 11 (*a*). Fluid injection shifts the intensity maximum toward the tube axis, as is also seen in figure 11 (*a*). In general, the region of maximum turbulent kinetic energy production has been found to lie near the maximum in turbulence intensity (Hinze 1959). In this light, the fact that the turbulence intensity in the annular region undergoes a substantial initial increase in the streamwise direction seems to be due to strong turbulence production therein.

## 4. Concluding remarks

The effects of injection on the structure of an initially fully developed, low Reynolds number turbulent tube flow have been studied by means of a hot-film anemometer. The observed results of the investigation and their interpretation are summarized in the following paragraphs.

Near the tube wall, the initial effect of injection is a significant reduction of the intensity of the axial turbulence fluctuations and an increase in the thickness of the viscous and buffer layers. The degree by which turbulence is suppressed in this region is more or less proportional to the ratio of the injection to entrance Reynolds numbers. As the flow moves downstream through the pipe the artificially thickened viscous layer rapidly becomes unstable, and the near-laminar flow in this region undergoes re-transition to fully developed turbulence.

In the core region of the flow, which is centred about the tube axis, there is also an initial reduction in the magnitude of $u'$, but to a lesser extent than that which occurs near the wall. This reduction is believed to be caused by the injection-induced acceleration of the flow. At larger values of $x/D$, $u'$ begins to increase,

presumably because of the transport of turbulence from the annular region of the flow toward the tube centre-line.

In the annular region separating the wall and core regions of the flow (that is, for those combinations of $Re_0$ and $Re_w$ which exhibit a distinct annular region) there is, initially, an increase in the magnitude of $u'$. This increase is believed to be due to an excess of turbulent energy production compared with the rate at which turbulent energy can be transported to other regions of the flow.

At higher values of the $Re_w/Re_0$ ratio, double maxima were observed in the $u'$ profiles in the portion of the tube where the flow is undergoing re-transition to fully developed turbulence.

This research was supported by Project N00014-68-A-0141-0001, administered by the Office of Naval Research.

## REFERENCES

BATCHELOR, G. K. 1953 *The Theory of Homogeneous Turbulence*, p. 68. Cambridge University Press.

ECKERT, E. R. G. & RODI, W. 1968 Reverse transition turbulent–laminar for flow through a tube with fluid injection. *J. Appl. Mech.* **35**, 817.

HINZE, J. O. 1959 *Turbulence*. McGraw-Hill.

HUESMANN, K. & ECKERT, E. R. G. 1968 Untersuchungen über die laminare Strömung und den Umschlag zur Turbulenz in porösen Rohren mit gleichmässiger Einblasung durch die Rohrwand. *Wärme- und Stoffübertragung*, **1**, 2.

OLSON, R. M. 1964 Experimental studies of turbulent flow in a porous circular tube with uniform mass transfer through the tube wall. Ph.D. thesis, University of Minnesota.

PENNELL, W. T. 1970 The effect of uniform mass injection on the structure of turbulent flow through a porous tube. Ph.D. thesis, University of Minnesota.

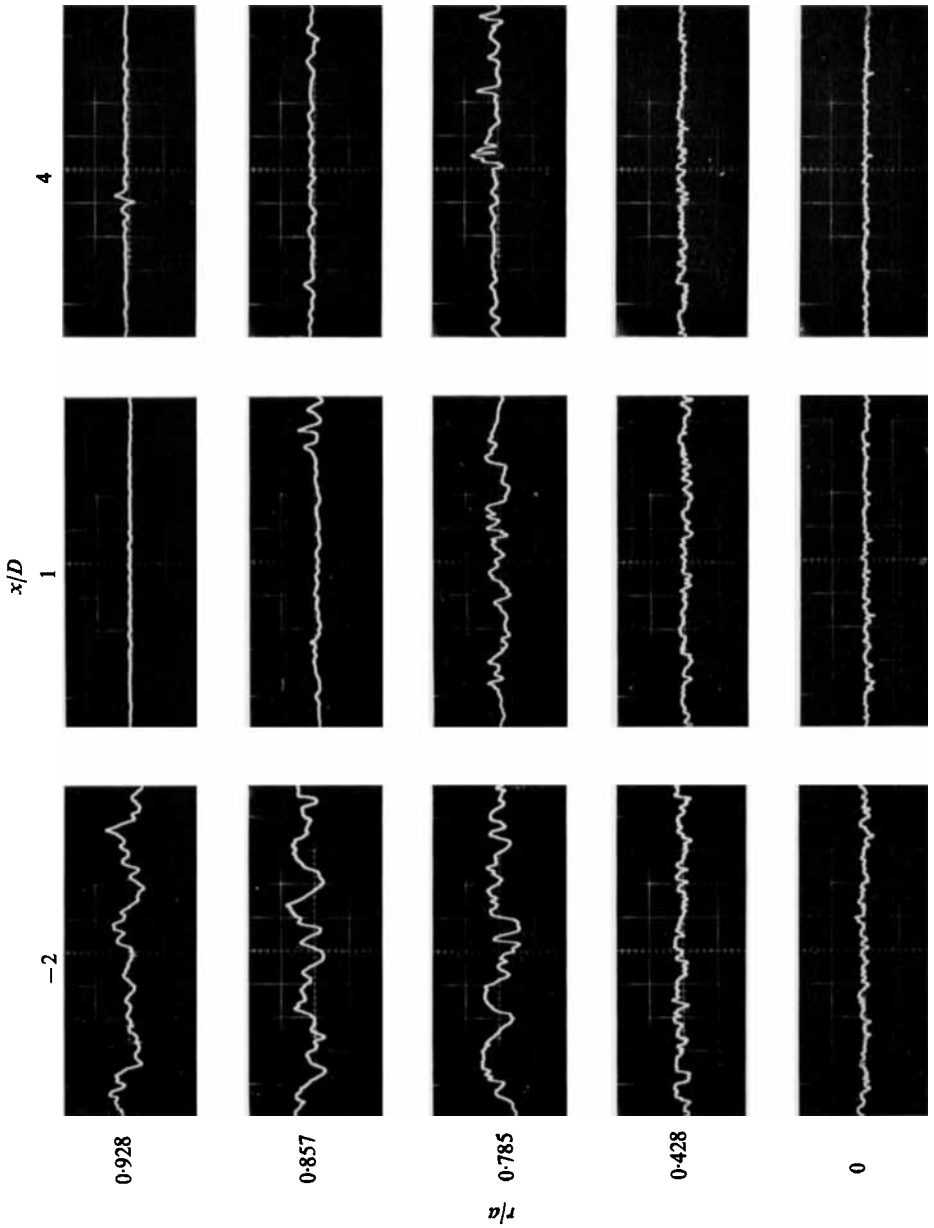


FIGURE 5. Photographs of oscilloscope traces showing the output of the hot-film sensor. $Re_0 = 3200$, $Re_w = 160$. (*a*) Entrance region. (*b*) Downstream region.

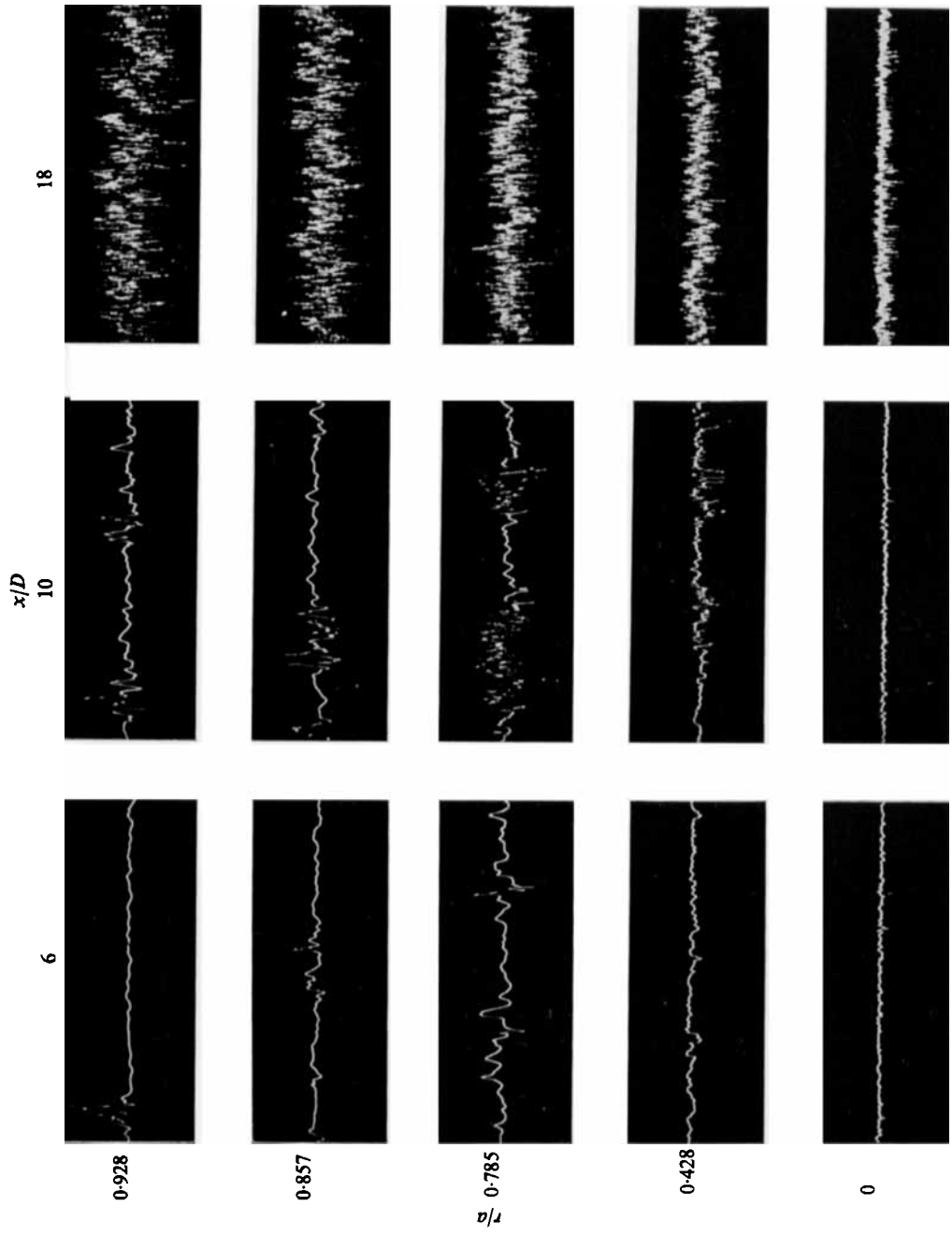


(*b*)

FIGURE 5. For legend see previous page.

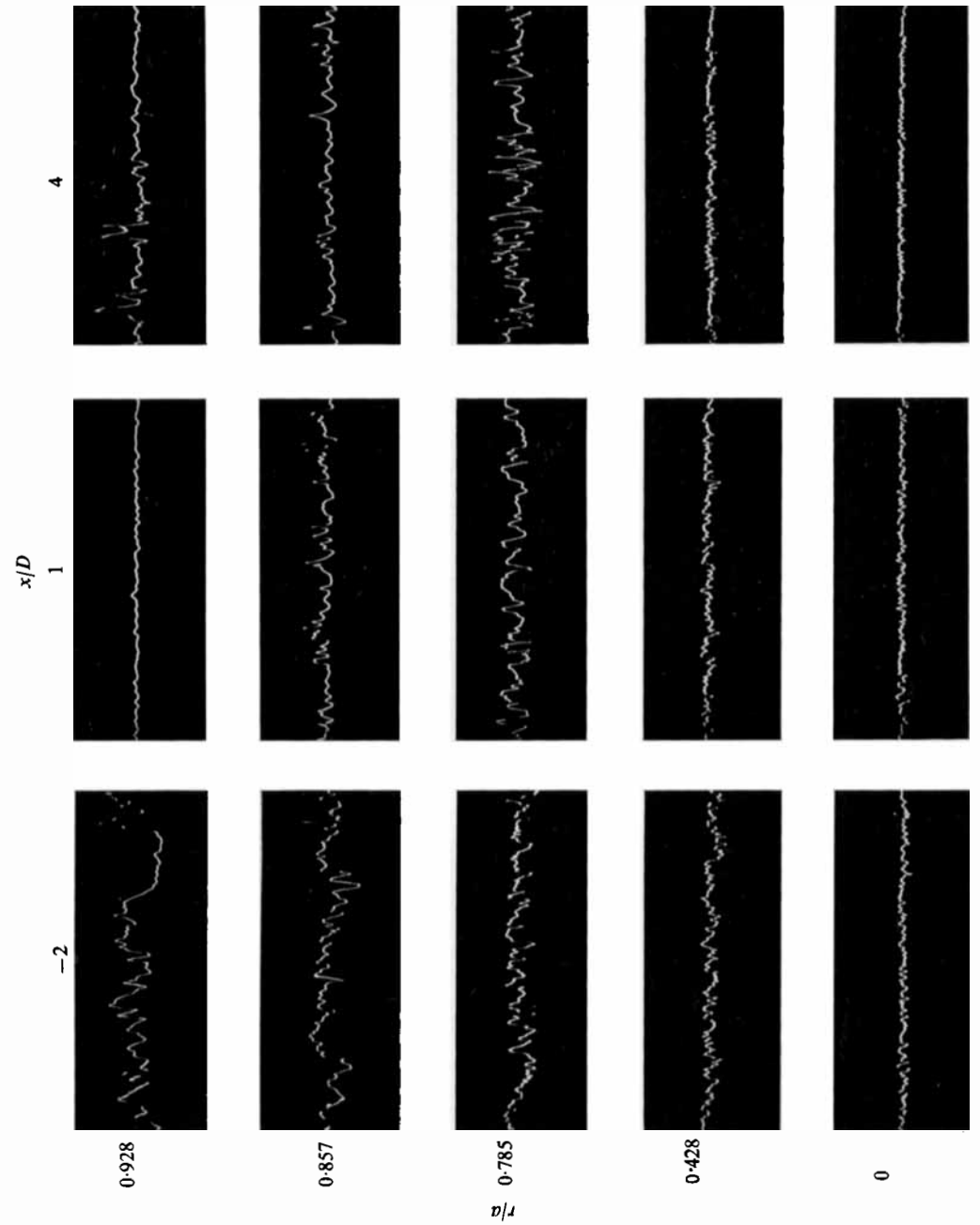


FIGURE 6. Photographs of oscilloscope traces showing the output of the hot-film sensor. $Re_0 = 4200$, $Re_w = 160$. (*a*) Entrance region. (*b*) Downstream region.

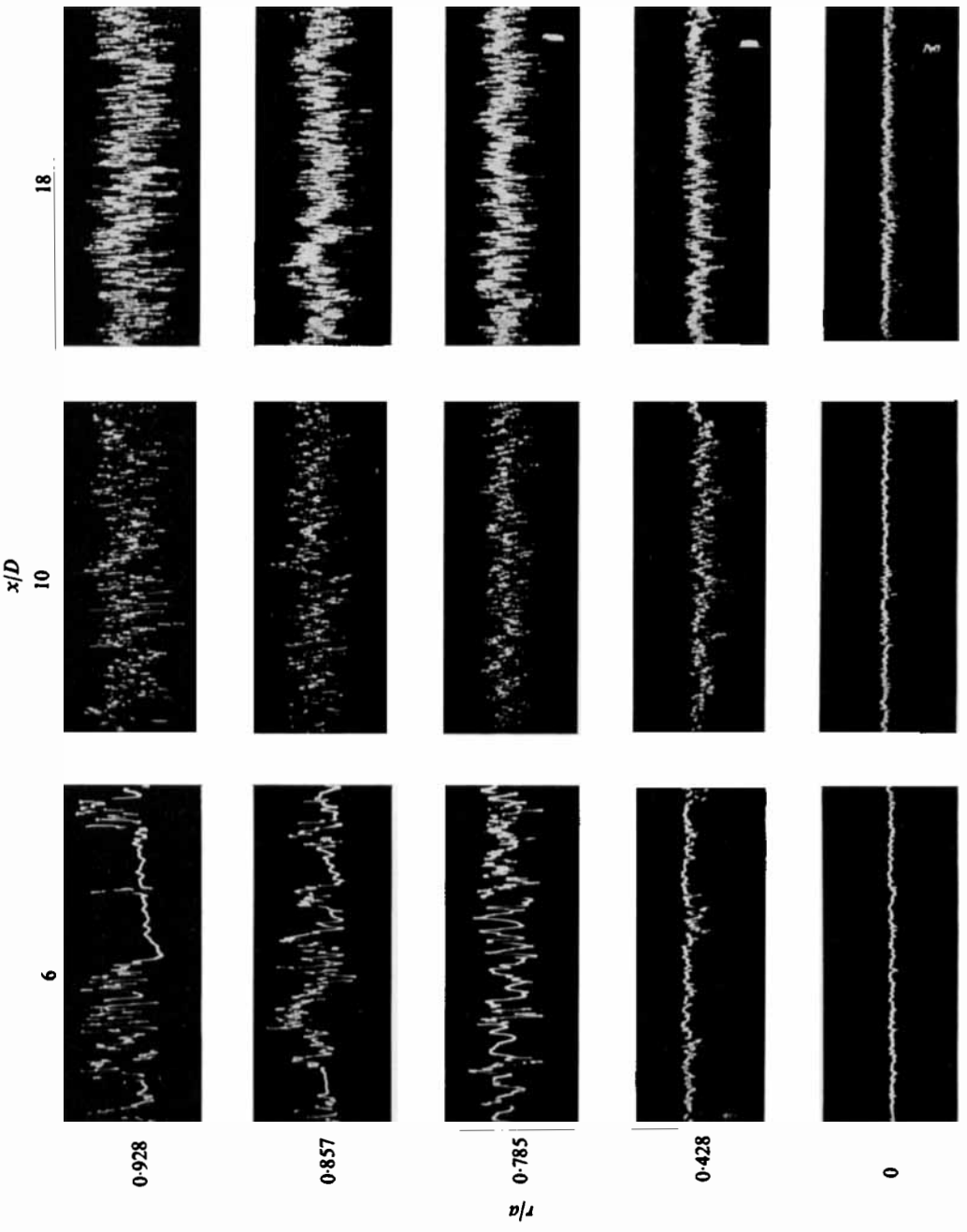


FIGURE 6. For legend see previous page.